

See discussions, stats, and author profiles for this publication at: <https://www.researchgate.net/publication/262492413>

# Detection of oxygen addition peaks for terpendole E and related indole–diterpene alkaloids in a positive–mode ESI–MS

ARTICLE *in* JOURNAL OF MASS SPECTROMETRY · JUNE 2014

Impact Factor: 2.38 · DOI: 10.1002/jms.3360

CITATION

1

READS

52

8 AUTHORS, INCLUDING:



[Yayoi Hongo](#)

Tata Elxsi

25 PUBLICATIONS 172 CITATIONS

[SEE PROFILE](#)



[Takemichi Nakamura](#)

RIKEN

27 PUBLICATIONS 535 CITATIONS

[SEE PROFILE](#)



[Takayuki Motoyama](#)

RIKEN

44 PUBLICATIONS 936 CITATIONS

[SEE PROFILE](#)



[Hiroyuki Osada](#)

RIKEN

482 PUBLICATIONS 10,359 CITATIONS

[SEE PROFILE](#)

# Detection of oxygen addition peaks for terpendole E and related indole–diterpene alkaloids in a positive-mode ESI-MS



This report describes that a regular positive electrospray ionization mass spectrometry (MS) analysis of terpendoles often causes unexpected oxygen additions to form  $[M + H + O]^+$  and  $[M + H + 2O]^+$ , which might be a troublesome in the characterization of new natural analogues. The intensities of  $[M + H + O]^+$  and  $[M + H + 2O]^+$  among terpendoles were unpredictable and fluctuated largely. Simple electrochemical oxidation in electrospray ionization was insufficient to explain the phenomenon. So we studied factors to form  $[M + H + O]^+$  and  $[M + H + 2O]^+$  using terpendole E and natural terpendoles together with some model indole alkaloids. Similar oxygen addition was observed for 1,2,3,4-tetrahydrocyclopent[b]indole, which is corresponding to the substructure of terpendole E. In tandem MS experiments, a major fragment ion at  $m/z$  130 from protonated terpendole E was assigned to the substructure containing indole. When the  $[M + H + O]^+$  was selected as a precursor ion, the ion shifted to  $m/z$  146. The same 16 Da shift of fragments was also observed for 1,2,3,4-tetrahydrocyclopent[b]indole, indicating that the oxygen addition of terpendole E took place at the indole portion. However, the oxygen addition was absent for some terpendoles, even whose structure resembles terpendole E. The breakdown curves characterized the tandem MS features of terpendoles. Preferential dissociation into  $m/z$  130 suggested the protonation tendency at the indole site. Terpendoles that are preferentially protonated at indole tend to form oxygen addition peaks, suggesting that the protonation feature contributes to the oxygen additions in some degrees. © 2014 The Authors. *Journal of Mass Spectrometry* published by John Wiley & Sons, Ltd.

Additional supporting information may be found in the online version of this article at the publisher's web site.

**Keywords:** terpendoles; indole–diterpene alkaloids; ESI oxidation; protonation site; oxygen addition for indole

Dear Sir,

Terpendoles, which are indole–diterpene alkaloids discovered from a soil-isolated fungal strain, were initially reported as inhibitors of acyl-CoA:cholesterol acyltransferase.<sup>[1,2]</sup> Terpendole E (Compound 1, Fig. 1) was re-discovered as a novel Eg5 inhibitor.<sup>[3]</sup> Some analogues have been regarded as candidates for lead compounds of anticancer drugs. For that reason, they are becoming attractive targets of chemical and biological research. Elucidation of molecular formulae with accurate mass measurement using mass spectrometry is the first task to distinguish and characterize analogues. Furthermore, hyphenation with liquid chromatography electrospray ionization mass spectrometry (LC-ESI-MS) is a sensitive identification technique that is useful for the analysis of terpendoles in a culture broth with far fewer preparation steps than those used for other techniques, such as X-ray diffraction and NMR analysis. However, unexpected  $[M + H + 16]^+$  and  $[M + H + 32]^+$  were often detected for terpendoles in a regular ESI-MS. Exact mass analyses defined them as one or two oxygen additions (Table 1). Undesirable oxygen additions cause mistakes in characterization and reduce the targeted ion signal intensity. It is also troublesome that the intensities of  $[M + H + O]^+$  and  $[M + H + 2O]^+$  fluctuated greatly and that they are unpredictable in each analysis. Simple electrochemical oxidation in ESI could not explain the observation as described later. Therefore, we studied factors affecting the formation of  $[M + H + O]^+$  and  $[M + H + 2O]^+$  using terpendole E and related natural indole–diterpenes together with some model indole alkaloids.

Electrospray ionization mass analysis of terpendole E (1) caused  $[M + H]^+$  ( $m/z$  438) with  $[M + H + O]^+$  ( $m/z$  454),  $[M + H + 2O]^+$  ( $m/z$  470) (Fig. 2(1)). Under the same regular ESI conditions, the oxygen addition peaks were observed at least for emindole SB

(2), terpendole I (3) and paspalline (4). All their spectra were shown in Supporting Information 1 with similar results of four model compounds:  $\alpha$ -paxitriol (5), androsterone derivative alcohol (7), 1,2,3,4-tetrahydrocyclopent[b]indole (9) and 1,2,3,4-tetrahydrocarbazole (10). An LC-MS succeeded in a separation of an isobaric impurity of the oxygen addition peak assigned to  $[(M + 2O) + H]^+$ , which increased in analyses for a preserved sample solutions with a time course of a few months (Supporting Information 2).

In this study, terpendoles (1, 2, 3 and 4) were extracted and purified from the culture broth as reported previously.<sup>[4]</sup>  $\alpha$ -Paxitriol (5) was prepared by chemical reduction of purchased paxilline (6) (Sigma-Aldrich Corp.).<sup>[5]</sup> Two simple steroidal indole alkaloids, alcohol (7) and ketone (8), were synthesized from androsterone in our laboratory. The detailed procedures are presented in Supporting Information 3. Yohimbine (11), reserpine (12), 1,2,3,4-tetrahydrocyclopent[b]indole (9) and 1,2,3,4-tetrahydrocarbazole (10) were purchased from Sigma-Aldrich Corp. and used without purification. For the ESI experiment, LC-MS grade methanol and water (Kanto Chemical Co. Inc) were used. Sodium formate was purchased from Sigma-Aldrich and Wako Pure Chemical Inds. Ltd. Special grade toluene (Wako Pure Chemical Industries. Ltd.) was dried using molecular sieve.

All LC-ESI-MS analyses in this study were conducted (Synapt G2 HDMS; Waters Corp., Manchester, UK) with a regular ESI-source

\* Correspondence to: Yayoi Hongo, RIKEN GRC, 2-1, Hirosawa, Wako, Saitama 351-0198, Japan. E-mail: yayoi@riken.jp

This is an open access article under the terms of the Creative Commons Attribution-NonCommercial-NoDerivs License, which permits use and distribution in any medium, provided the original work is properly cited, the use is non-commercial and no modifications or adaptations are made.

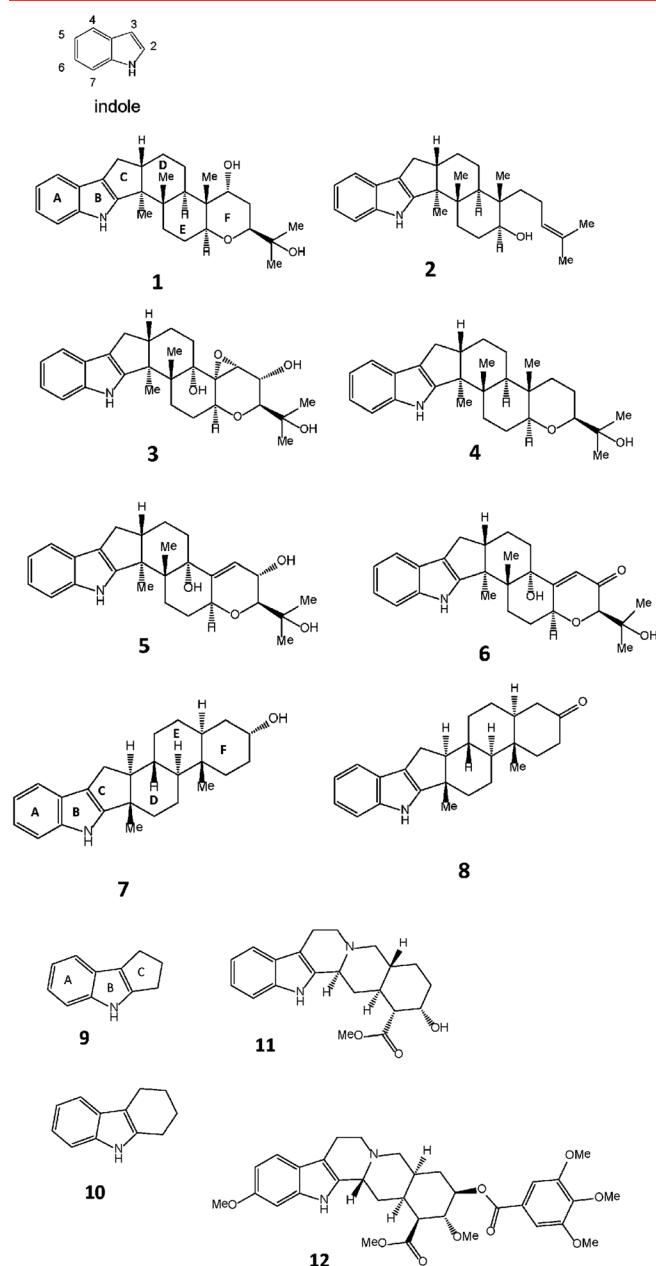


**Figure 1.** Structures of 12 compounds including five natural terpendoles and seven model compounds: **1**, terpendole E; **2**, emindole SB; **3**, terpendole I; **4**, paspaline; **5**,  $\alpha$ -paxitriol; **6**, paxilline; **7**, alcohol; **8**, ketone; **9**, 1,2,3,4-tetrahydrocyclopent[b]indole; **10**, 1,2,3,4-tetrahydrocarbazole; **11**, yohimbine; **12**, reserpine.

unit, but the oxygen additions on terpendoles are also observed by another device (4000 Q Trap LC-MS system; AB Sciex) with a turbo spray ion source. Isocratic LC separation system (Acquity; Waters Corp.) with 20% water and 80% methanol at a flow rate of 300  $\mu$ L/min. A BEH C<sub>18</sub> column (2.1  $\times$  50 mm, 1.7  $\mu$ m) at 40 °C for the separation. The time-of-flight analyzer was set for resolution-mode with resolving power of 20 000 at  $m/z$  556 (leucine enkephalin). The  $m/z$  range of 100–1500 was calibrated using 100 ppm sodium formate solution. The desolvation temperature was fixed at 250 °C. Regular ESI conditions in this study were set to obtain the maximum intensity of  $[M+H]^+$  for terpendole E; a stainless steel ESI capillary was applied high voltage of 3.0 kV, and the cone and desolvation gas ( $N_2$ ) flows were set to 200 l/h

**Table 1.** Observed accurate masses of terpendoles and analogues

Compound	Formula	$[M+H]^+$			$[M+H+O]^+$			$[M+H+2O]^+$		
		Theoretical	Observed	Error	Theoretical	Observed	Error	Theoretical	Observed	Error
Terpendole E ( <b>1</b> )	$C_{28}H_{39}NO_3$	438.3008	438.3002	–1.4	454.2957	454.2962	0.5	470.2906	470.2914	0.8
Emindole SB ( <b>2</b> )	$C_{28}H_{39}NO$	406.3110	406.3113	0.7	422.3059	422.3067	0.8	438.3008	438.3011	0.3
Terpendole I ( <b>3</b> )	$C_{27}H_{35}NO_5$	454.2593	454.2585	–1.8	470.2542	470.2540	–0.2	486.2491	486.2484	–0.7
Paspaline ( <b>4</b> )	$C_{28}H_{39}NO_2$	422.3059	422.3058	–0.2	438.3008	438.2997	–1.1	454.2957	454.2948	–0.9
$\alpha$ -Paxitriol ( <b>5</b> )	$C_{27}H_{35}NO_4$	438.2644	438.2640	–0.4	454.2593	454.2595	0.2	470.2543	470.2549	0.6
Paxilline ( <b>6</b> )	$C_{27}H_{33}NO_4$	436.2488	436.2480	–0.8	452.2437	—	—	468.2386	—	—
Alcohol ( <b>7</b> )	$C_{25}H_{33}NO$	364.2640	364.2643	0.3	380.2589	380.2575	–1.4	396.2538	396.2533	–0.5
Ketone ( <b>8</b> )	$C_{25}H_{33}NO$	362.2484	362.2481	–0.3	378.2433	—	—	394.2382	—	—
1,2,3,4-Tetrahydrocyclopent[b]indole ( <b>9</b> )	$C_{11}H_{11}N$	158.0970	158.0972	0.2	174.0919	174.0921	0.2	190.0866	190.0872	0.6
1,2,3,4-Tetrahydrocarbazole ( <b>10</b> )	$C_{12}H_{13}N$	172.1126	172.1125	–0.1	188.1075	188.1076	0.1	204.1024	204.1026	0.2
Yohimbine ( <b>11</b> )	$C_{21}H_{26}N_2O_3$	355.2022	355.2019	–0.3	371.1971	—	—	387.1920	—	—
Reserpine ( <b>12</b> )	$C_{33}H_{40}N_2O_9$	609.2812	609.2816	0.4	625.2761	—	—	641.2711	—	—

\* R.Int. relative intensity normalized to the intensity of  $[M+H]^+$ .

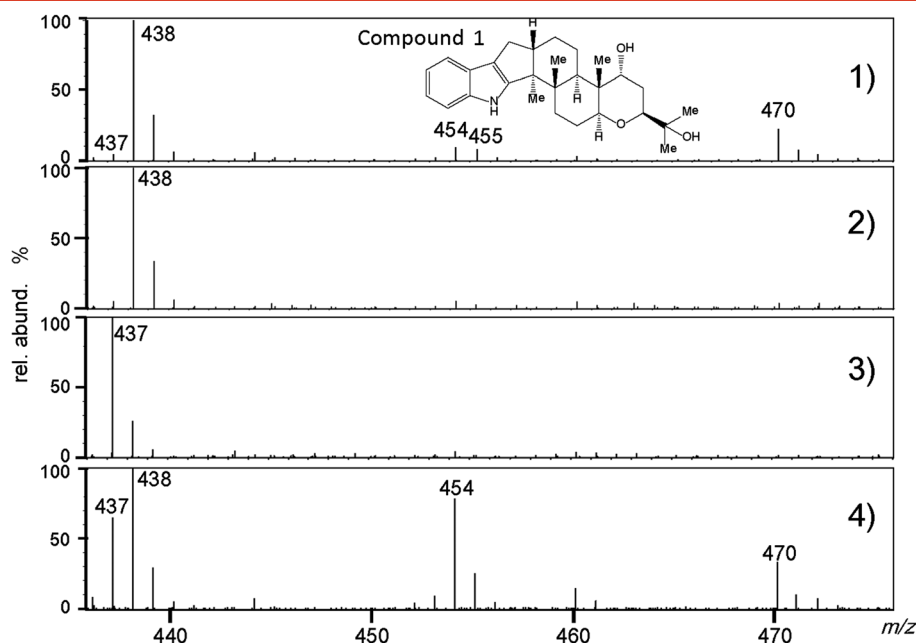


**Figure 2.** Mass spectra of terpendole E: (1) under regular conditions, with cone and desolvation gas settings of 200 l/h and 300 l/h, respectively.  $[M + \text{NH}_4]^+$  was detected at  $m/z$  455. (2) Hydroquinone addition (300 ppm); (3) using dry toluene as a working solvent; and (4) cone and desolvation gas settings of 80 l/h and 100 l/h.

and 300 l/h, respectively. Samples were set as 5 ppm; 5  $\mu\text{l}$  of the solution was injected into the system. The tandem MS (MS/MS) experiments were conducted with collision-induced dissociation technique with laboratory collision energies at 20 or 25 V. Precursor ions of interest were isolated using a Q mass analyzer with a 1 u mass isolation window (high-resolution setting) for  $[M + \text{H}]^+$  to separate them from  $[M]^+$ . Ions were let through the collision-induced dissociation cell where  $\text{Ar } 2.44 \times 10^{-2} \text{ e}^{-2} \text{ mbar}$  was filled as the collision gas.

Hydroquinone is known as one of redox buffers that partially participate directly in the neutralization of free radicals and reactive oxygen species.<sup>[6,7]</sup> With the addition of hydroquinone (300 ppm in resultant solution),  $[M + \text{H} + \text{O}]^+$  and  $[M + \text{H} + 2\text{O}]^+$  formation are suppressed in the terpendole E (1) analysis (Fig. 2 (2)). It indicated that the reactive oxygen formed by the oxidation process in ESI causes the oxygen addition for terpendole E. Using dry toluene as a solvent, the oxygen addition was diminished, and  $[M]^+$  ( $m/z$  437) became prominent (Fig. 2(3)). To confirm the origin of the oxygen, incorporation experiment using  $^{18}\text{O}$ -labeled water was performed in the  $\alpha$ -paxitriol analysis. Isotope labeled water was added into the post-column flow through line, and a new peak was observed at  $m/z$  474 (obs. 474.2620) assigned to  $[M + \text{H} + 2^{18}\text{O}]^+$  (calc. 474.2627) for  $\alpha$ -paxitriol (5) (Supporting Information 4). Hence, we concluded that the additional oxygen originated from water in the solvent system. Reactive oxygen formation from water is the most favorable reaction because of the low oxidation potentials ( $2\text{H}_2\text{O} = \text{O}_2 + 4\text{H}^+ + 4\text{e}^-$  ( $E_0(2\text{H}^+/\text{H}_2) = 1.25 \text{ V}$ )). Successive formation of reactive oxygen species (such as  $\text{H}_2\text{O}_2$  ( $2\text{OH}^- = \text{H}_2\text{O}_2 + 2\text{e}^-$ )) can also take place via electrolysis.<sup>[8]</sup> Obvious mass shift (2 Da) was absent for  $[M + \text{H} + \text{O}]^+$  by the addition of  $^{18}\text{O}$ -water. It might be a result from the insufficient formation of  $[M + \text{H} + \text{O}]^+$  and isobaric interference of the isotope of  $[M + \text{NH}_4]^+$  on  $[M + \text{H} + ^{18}\text{O}]^+$ .

The anodic side reaction of analytes in positive-mode ESI has been well documented for alkylation and polymerization of phenylenediamines,<sup>[9,10]</sup> gas-phase methanol addition of aromatic aldehydes<sup>[11]</sup> and halogen addition to  $\pi$ -conjugated

phosphasilenes.<sup>[12]</sup> Multiple electrochemical parameters, containing material of capillary metal, flow rate, needle voltage and gas flows, contribute to the reactions. Oxygen additions to the compound in positive-mode ESI were also documented for reserpine<sup>[13]</sup> and zotepine<sup>[14]</sup> with some byproducts using potentiostat system incorporated into ESI system. Without potentiostat system, no oxidized ions were observed for yohimbine (11) and reserpine (12) under any ESI settings in this study (Supporting Information 5(1 and 2)). Therefore, the molecular feature of terpendoles partially contributed on the oxygen addition as well as electrochemical formation of reactive oxygen. However, the structural character that causes oxygen additions in ESI has only rarely been understood. Reduction of both cone and desolvation gas flows increased the signal of oxygen additions for terpendole E (Fig. 2(4)), indicating that the balance of gas parameter settings was one of controlling factors. On the other hand, no systematic trend was observed between the needle voltage setting and the relative intensities of oxygen addition peaks for terpendole E (1) (Supporting Information 6). The parameters giving the maximum intensity of  $[M + \text{H} + \text{O}]^+$  or  $[M + \text{H} + 2\text{O}]^+$  varied among compound. To compare the degrees of oxygen additions among structures, we examined the identical regular ESI condition on the indole containing compounds (Table 1, Supporting Information 1 and 6). The smallest compound that gave the oxygen additions under the regular ESI settings was 1,2,3,4-tetrahydrocyclopent[*b*] indole (9). Also, 1,2,3,4-tetrahydrocarbazole (10) gave the oxygen addition peaks  $[M + \text{H} + \text{O}]^+$  and  $[M + \text{H} + 2\text{O}]^+$  with intense  $[M + \text{O}]^+$ . The oxygen additions for 1,2,3,4-tetrahydrocyclopent[*b*] indole (9) and 1,2,3,4-tetrahydrocarbazole (10) are favorable to take place at reactive C-2 and C-3 positions of indole.<sup>[15]</sup>

To elucidate the oxidation site of terpendole E, MS/MS experiments were conducted on  $[M + \text{H}]^+$  and the oxygen added peaks. Protonated terpendole E (1) ( $[M + \text{H}]^+$  at  $m/z$  438) was fragmented into  $m/z$  130 (130.0660) attributed to 3-methyleneindolium or N-protonated quinoline ion ( $\text{C}_9\text{H}_8\text{N}^+$ , calc. 130.0657),<sup>[16]</sup> which was

identical fragment ion observed for MS/MS on protonated 1,2,3,4-tetrahydrocyclopent[b]indole (**9**) (Fig. 3). When the  $[M+H+O]^+$  was selected as the precursor ion,  $m/z$  130 of both terpendole E (**1**) and 1,2,3,4-tetrahydrocyclopent[b]indole (**9**) shifted to  $m/z$  146 (146.0595,  $C_9H_8NO^+$  calc. 146.0606). The MS/MS on  $[M+H+2O]^+$  also gave fragment ions assigned to oxidized 3-methyleneindolium or *N*-protonated quinoline ion for both compounds. The peak at  $m/z$  145 (145.0519) from  $[M+H+2O]^+$  of 1,2,3,4-tetrahydrocyclopent[b]indole (**9**) was assigned to  $C_9H_7NO^+$  (calc. 145.0528), containing oxidized indole. These observations indicated that the site of the oxygen additions of terpendole E (**1**) was indole portion same as that of 1,2,3,4-tetrahydrocyclopent[b]indole (**9**).

Terpendole E (**1**) is composed with some ring units; indole part with rings A, B and diterpene part from ring C to the tetrahydropyran ring F, which connects with fused cyclopentene ring C. (Fig. 1). The ring A–C portion can be recognized as the substructure of indole fused with cyclopentene ring C at C-2 and C-3 double bond of the indole. Two hydroxyl groups exist on the tetrahydropyran ring F and a 2-hydroxyisopropyl side chain of the ring F. The resemblance of oxygen addition and MS/MS features of terpendole E to 1,2,3,4-tetrahydrocyclopent[b]indole (**9**) suggested that the ring A–C portion of terpendole E (**1**) was a significant structure in the oxidation reaction.

It is particularly interesting that the oxygen additions were rarely detected for some terpenoids, even having an identical ring A–C structure. Paxilline (**6**) possesses a conjugated ketone carbonyl group in dihydropyran ring F (Supporting Information 6 (3)). Although small oxygen addition peaks were detected with changing condition from regular ESI, the intensities of both  $[M+H+O]^+$  and  $[M+H+2O]^+$  of protonated paxilline (**6**) were smaller than those of  $\alpha$ -paxitriol (**5**), which was a reduction product of paxilline (**6**) having an  $\alpha$ -oriented hydroxyl group at the allylic position in ring F. The core structures were unchanged; however, fragmentation characteristics described by means of breakdown curves in MS/MS experiments showed the significant difference between them. Fragment ion at  $m/z$  130 was characteristic for  $\alpha$ -paxitriol (**5**) (Fig. 4(a)). On the

other hand, a water loss competed to the formation of  $m/z$  130 for paxilline (**6**) (Fig. 4(b)). Preferential fragmentation into  $m/z$  130 required protonation at the indole portion for  $\alpha$ -paxitriol (**5**), and a water loss of protonated paxilline (**6**) should be triggered by the proton localization at a hydroxyl group in the ring D–F portion. For paxilline (**6**), proton can migrate into the hydroxyl group on the 2-hydroxyisopropyl group followed by the first protonation at the carbonyl site at the ring F via 6-membered ring intermediate. Available data of gas-phase proton affinities predict the favorable protonation site in the terpenoids. Proton affinities of indole and alkyl ketone were reported to be 891–986 kJ/mol<sup>[16–19]</sup> and up to 864 kJ/mol,<sup>[18]</sup> respectively. Their comparable proton affinities in paxilline (**6**) could cause the competitive proton localization between the ring A–C portion and the ring D–F portion with a ketone. However, if the ring D–F portion contained only hydroxyl group like  $\alpha$ -paxitriol (*i*-C<sub>3</sub>H<sub>7</sub>OH: 793 kJ/mol<sup>[18]</sup>), a proton should localize at the indole preferentially because of its higher proton affinity.

Therefore, we can assume the additional factor to facilitate the oxygen additions; preferential localization of a charged proton at the indole portion as well as 1,2,3,4-tetrahydrocyclopent[b]indole (**9**). Although the reaction mechanism to add oxygen to protonated indole has not been clear yet, the structure containing the ring A–C portion may be insufficient to the substantial reaction.

In the same way, oxygen additions were observed for alcohol (**7**), but absent for ketone (**8**). Although the protonated (**8**) fragmented into  $m/z$  130 predominantly as well as (**7**), higher energy was necessary to give the fragment than (**7**) (Fig. 4(c) and 4(d)). If the behavior upon protonation was identical between these two, the energy requirements to form  $m/z$  130 should be similar. The comparable proton affinities between indole and ketone group at ring F for compound (**8**) could reduce the population of indole protonated species rather than the case of compound (**7**).

The artificial oxygen additions to terpenoids in positive ESI-MS were described here. Multiple factors control the phenomenon: water contents in the ESI system, oxidation of water to form reactive oxygen species, and protonation site of molecules. To

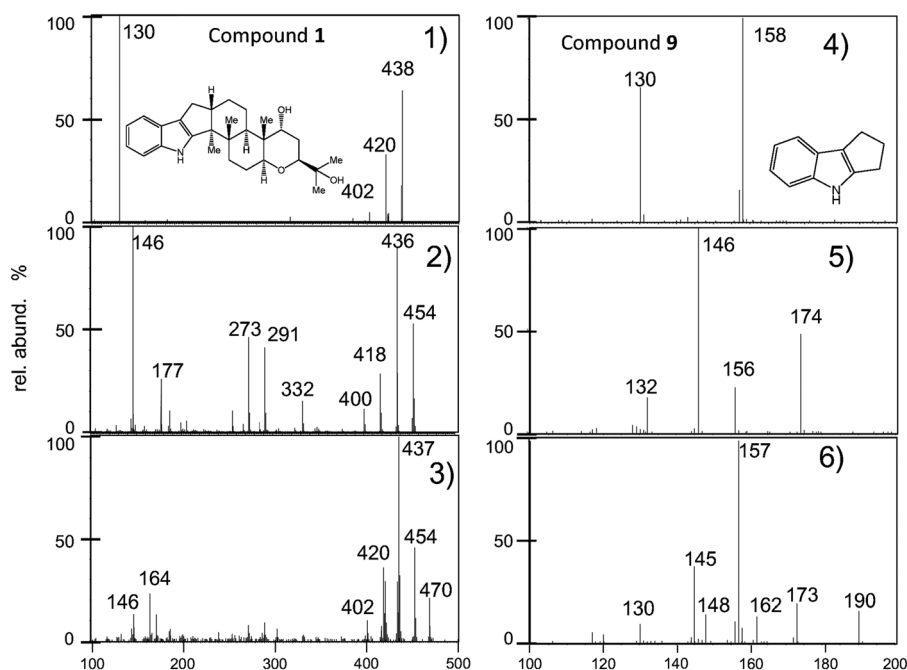


**Figure 3.** Tandem mass spectrometry spectra of terpendole E: (1)  $[M+H]^+$  (collision energy = 20 V), (2)  $[M+H+O]^+$  (20 V), (3)  $[M+H+2O]^+$  (25 V) and 1,2,3,4-tetrahydrocyclopent[b]indole: (4)  $[M+H]^+$  (20 V), (5)  $[M+H+O]^+$  (20 V), (6)  $[M+H+2O]^+$  (25 V).



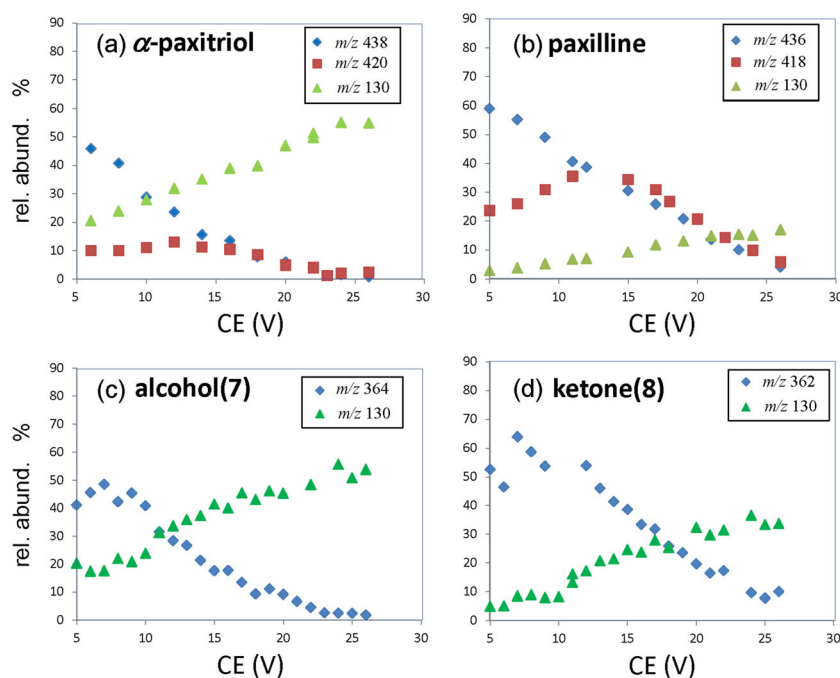


**Figure 4.** Breakdown curves of protonated ions: (a)  $\alpha$ -paxitriol, (b) paxilline, (c) alcohol(7) and (d) ketone(8). (Closed rhombus denoted precursor ions. Closed triangle denoted the fragment ion at  $m/z$ 130. Closed cube in (a) and (b) denoted the water-loss fragment ions.

reduce the unexpected oxygen addition as possible, hydroquinone addition after LC separation is expected to be one of effective means. The oxygen additions also depend on the analyte structure. Protonation at indole portion of the terpendole structure seemed to be the key to the oxygen addition. Unfortunately, it would be difficult to control protonation site for compounds in each ESI settings, but source tuning to give dominant  $[M]^+$  or  $[M+Na]^+$  formation may also be effective to reduce unexpected ions.

### Acknowledgements

This work was partly supported by Grants-in-Aid from the Ministry of Education, Culture, Sports, Science and Technology, Japan. This study was also supported in part by the Program for Promotion of Basic and Applied Researches for Innovations in Bio-oriented Industry.

Yours,

Yayoi Hongo,<sup>a\*</sup> Takemichi Nakamura,<sup>a</sup> Shunya Takahashi,<sup>a</sup> Takayuki Motoyama,<sup>b</sup> Toshiaki Hayashi,<sup>b</sup> Hiroshi Hirota,<sup>b</sup> Hiroyuki Osada<sup>b,c</sup> and Hiroyuki Koshino<sup>a,d</sup>

<sup>a</sup>Global Research Cluster, RIKEN, Wako, Japan

<sup>b</sup>Antibiotics Laboratory, RIKEN, Wako, Japan

<sup>c</sup>Center for Sustainable Resource Science, RIKEN, Wako, Japan

<sup>d</sup>Synthetic Organic Chemistry Laboratory, RIKEN, Wako, Japan

### References

- [1] X.-H. Huang, H. Nishida, H. Tomoda, N. Tabata, K. Shiomi, D.-J. Yang, H. Takayanagi, S. Ōmura. Terpendoles, novel ACAT inhibitors produced by *Albophoma yamanashiensis*. II. Structure elucidation of terpendoles A, B, C and D. *J. Antibiotics* **1995**, 48, 5.
- [2] H. Tomoda, N. Tabata, D. J. Yang, H. Takayanagi, S. Ōmura. Terpendoles, novel ACAT inhibitors produced by *Albophoma yamanashiensis*. III. Production, isolation and structure elucidation of new components. *J. Antibiotics* **1995**, 48, 793.
- [3] J. Nakazawa, J. Yajima, T. Usui, M. Ueki, A. Takatsuki, M. Imoto, Y. Toyoshima, H. Osada. A novel action of terpendole E on the motor activity of mitotic kinesin Eg5. *Chemistry and Biology* **2003**, 10, 131.
- [4] T. Motoyama, T. Hayashi, H. Hirota, M. Ueki, H. Osada. Terpendole E, a kinesin Eg5 inhibitor, is a key biosynthetic intermediate of indole-diterpenes in the producing fungus *Chaunopycnis alba*. *Chemistry and Biology* **2012**, 19, 1611.
- [5] J. Penn, P. G. Mantle. Biosynthetic intermediates of indole-diterpenoid mycotoxins from selected transformation at C-10 of paxilline. *Phytochemistry* **1994**, 4, 921.
- [6] G. J. Van Berkel, V. Kertesz. Redox buffering in an electrospray ion source using a copper capillary emitter. *J. Mass Spectrom.* **2001**, 36, 1125.
- [7] S. Plattner, R. Erb, J. P. Chervet, H. Oberacher. Ascorbic acid for homogenous redox buffering in electrospray ionization-mass spectrometry. *Anal. Bioanal. Chem.* **2012**, 404, 1571.
- [8] G. J. Van Berkel, V. Kertesz. Using the electrochemistry of the electrospray ion source. *Anal. Chem.* **2007**, 79, 5510.
- [9] R. Abburi, S. Kalkhof, R. Oehme, A. Kiontke, C. Birkemeyer. Artifacts in amine analysis from anodic oxidation of organic solvents upon electrospray ionization for mass spectrometry. *Eur. J. Mass Spectrom.* **2012**, 18, 301.
- [10] F. L. Palmisano and P. G. Zamboni. O-phenylenediamine electropolymerization by cyclic voltammetry combined with electrospray ionization-ion trap mass spectrometry. *Anal. Chem.* **2003**, 75, 4988.
- [11] L. Wang, Y. Chai, P. Tu, C. Sun, Y. Pan. Formation of  $[M+15]^+$  ions from aromatic aldehydes by use of methanol: in-source aldolization reaction in electrospray ionization mass spectrometry. *J. Mass Spectrom.* **2011**, 46, 1203.
- [12] Y. Hongo, B. Li, K. Suzuki, T. Nakamura. An unexpected  $[M+I]^+$  ion formation in phosphasilene compounds detection by electrospray ionization mass spectrometry. *J. Mass Spectrom.* **2011**, 46, 956.
- [13] V. Kertesz, G. J. Van Berkel. Control of analyte electrolysis in electrospray ionization mass spectrometry using repetitively pulsed high voltage. *Int. J. Mass Spectrom.* **2011**, 303, 206.
- [14] K. Nozaki, H. Kitagawa, S. Kimura, A. Kagayama, R. Arakawa. Investigation of electrochemical oxidation products and their

- fragmentations of zotepine using on-line electrochemistry/electrospray ionization mass spectrometry. *J. Mass Spectrom.* **2006**, 41, 606.
- [15] R. J. Sundberg. The chemistry of indoles. V. Oxidation, Degradation, and Metabolism of the Indole Ring. Academic Press: NewYork - London **1970**, 282–315.
- [16] Z. You, C. Guo, Y. Pan. An experimental and theoretical study on fragmentation of protonated *N*-(2-pyridinylmethyl)indole in electrospray ionization mass spectrometry. *Rapid Commun. Mass Spectrom.* **2012**, 26, 2509.
- [17] Y. Huang, L. Liu, S. Liu. Towards understanding proton affinity and gas-phase basicity with density functional reactivity theory. *Chem. Physics. Lett.* **2012**, 527, 73.
- [18] E. P. L. Hunter, S. G. Lias. Evaluated gas phase basicities and proton affinities of molecules: an update. *J. Phys. Chem. Ref. Data* **1998**, 27, 413.
- [19] A. R. Dongré, J. L. Jones, Á. Somogyi, V. H. Wysocki. Influence of peptide composition, gas-phase basicity, and chemical modification on fragmentation efficiency: evidence for the mobile proton model. *J. Am. Chem. Soc.* **1996**, 118, 8365.

---

## Supporting information

Additional supporting information may be found in the online version of this article at the publisher's web site.